JCTC Journal of Chemical Theory and Computation

Modeling β-Scission Reactions of Peptide Backbone Alkoxy Radicals: Backbone C−C Bond Fission

Geoffrey P. F. Wood,[†,‡] Arvi Rauk,[§] and Leo Radom*[,†,‡]

School of Chemistry, University of Sydney, Sydney, New South Wales 2006, Australia, Research School of Chemistry, Australian National University, Canberra, ACT 0200, Australia, and Department of Chemistry, University of Calgary, Calgary, Alberta T2N IN4, Canada

Received May 17, 2005

Abstract: To model the C−C β-scission reactions of backbone peptide alkoxy radicals, enthalpies and barriers for the fragmentation of four substituted alkoxy radicals have been calculated with a variety of ab initio molecular orbital theory and density functional theory procedures. The high-level methods examined include CBS-QB3, variants of the G3 family, and W1. Simpler methods include HF, MP2, QCISD, B3-LYP, BMK, and MPW1K with a range of basis sets. We find that good accuracy can be achieved with the G3(MP2)//B3-LYP and G3X(MP2)-RAD methods. Lower-cost methods producing reasonable results are single-point energy calculations with UB3-LYP/6-311+G(3df,2p), RB3-LYP/6-311+G(3df,2p), UBMK/6-311+G(3df,2p), and RBMK/6-311+G(3df,2p) on geometries optimized with UB3-LYP/6-31G(d) or UBMK/6-31G(d). Heats of formation at 0 K for the alkoxy radicals and their fragmentation products were also calculated. We predict $\Delta_f H_0$ values for the alkoxy radicals of −71.4 ($^{\bullet}OCH_2$-CH=O), −102.5 ($^{\bullet}OCH(CH_3)CH=O$), −176.6 ($^{\bullet}OCH(CH_3)C(NH2)=O$), and −264.6 ($^{\bullet}OC(CH_3)$-(NHCH=O)CH=O) kJ mol^{-1}. For the fragmentation products $NH_2C(^{\bullet})=O$ and CH(=O)NHC-(CH_3)=O, we predict $\Delta_f H_0$ values of −5.9 kJ mol^{-1} and −352.8 kJ mol^{-1}.

1. Introduction

Radical-mediated protein damage has been implicated in a number of diseases such as Alzheimer's disease, atherosclerosis, and diabetes as well as aging.[1−3] Two general observations can be made concerning research dedicated to this subject.[1] First, there are a vast number of possible reactions due to the complexity of proteins and the variety in functionality of peptide residues. Second, the complexity of the species and the possibility of long chain lengths make experimental elucidation of specific processes difficult to achieve.

It has been postulated that alkoxy radicals may form on the peptide backbone via peroxyl radicals through a tetroxide. Alternatively, they may be generated by one-electron reduction of alkyl hydroperoxides or dialkyl peroxides.[1] Once the alkoxy radical (**1**) has formed on a peptide backbone, it may undergo one of three possible fragmentation reactions, namely fission of the C−C bond (A), fission of the C−N bond (B), or loss of the R_3 side-chain (C):

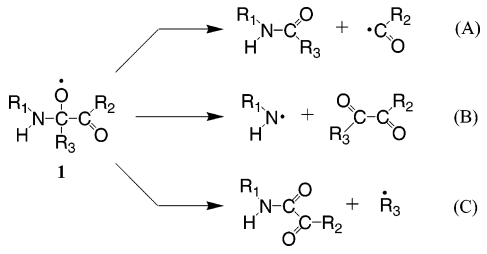

1

In general, alkoxy cleavage reactions have been found to be endothermic,[4] and the preferred pathway is generally determined by the stability of the radical that is formed.[5] However, this is not always the case, and for one particular class of ring-opening reactions,[6] that has been studied computation-

* Corresponding author e-mail: radom@chem.usyd.edu.au.
† University of Sydney.
‡ Australian National University.
§ University of Calgary.

10.1021/ct050133g CCC: $30.25 © 2005 American Chemical Society
Published on Web 08/05/2005

ally,[7] the most stable thermodynamic products are not formed. Other computational studies in this area include investigations of the associated β-scission reactions of a general series of alkoxy radicals.[8,9] Good agreement between theory and experiment was found for reaction enthalpies and heats of formation at the B3-LYP/SVP, CBS-RAD, and G2-(MP2) levels of theory. Dibble[10] has also carried out theoretical studies on cleavage reactions of isoprene-derived alkoxy radicals. Using B3-LYP with small and medium-sized basis sets as well as the CBS-4 and CBS-q model chemistries he found that the cleavage barriers were small.

In a recent study, Huang and Rauk[11] performed an initial investigation of the fragmentation reactions A, B, and C. In that study, the B3-LYP/6-31G(d) method was used to determine free energies of fragmentation for model systems containing an alanine and glycine residue. In the present study, we examine in more detail the pathway leading to C−C bond fission (A) using four models (A1−A4). We use both high-level ab initio procedures and simpler calculations to investigate their reaction enthalpies and barriers.

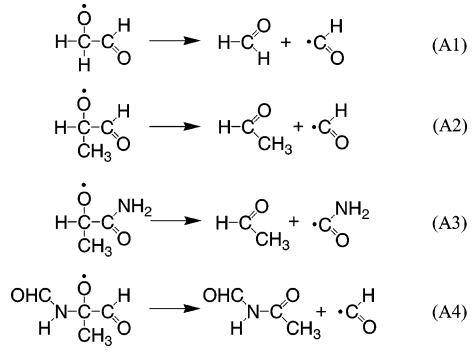

The first reaction, A1, represents the smallest system that can be used to model reaction A. It is clearly a very simplified model but it allows the assessment of a wide range of theoretical procedures. At the other extreme, reactions A3 and A4 represent more realistic models, but because of their increased size they are more restricted in the range of theoretical procedures that can be applied.

We also make high-level predictions of the heats of formation at 0 K for the alkoxy radicals and for the cleavage products of reactions A1−A4. Heats of formation for some of these species have been previously determined experimentally and computationally, and we use the new calculated values in these cases to further assess the performance of the various theoretical techniques. In other cases, we predict heats of formation for species for which the values are not currently known. For example, reactions A3 and A4 involve substituted alkoxy radicals that have not been studied theoretically before, and for which no thermodynamical data are currently available. On the other hand, the radical product $NH_2C(^{\bullet})=O$, formed in the cleavage reaction A3, has been previously studied theoretically in the context of combustion chemistry[12] and also in the examination of N−H bond energies.[13] However, an accurate heat of formation is lacking.

2. Theoretical Procedures

Standard ab initio molecular orbital theory[14] and density functional theory[15] calculations were carried out with the ACES II,[16] GAUSSIAN 98,[17] GAUSSIAN 03,[18] and MOLPRO 2002.6[19] computer programs.

Unless otherwise stated, calculations have been carried out using an unrestricted reference wave function. Calculations on radicals that have used a restricted-open-shell reference wave function are designated with an "R" prefix. Those that use the partial spin restriction of MOLPRO[20] have a "UR" prefix. We have employed the frozen-core approximation, except in cases where prescribed model chemistries, e.g. G3//B3-LYP,[21] require full calculations to be carried out.

Geometries were initially scanned using the B3-LYP/6-31G(d) level of theory. Geometry optimizations were then carried out at points on the scans that indicated equilibrium structures of reactants and products or transition structures for their interconversion. The optimizations were followed by vibrational frequency analyses to ensure that the selected structures correspond to minima (no imaginary frequencies) or saddle points (one imaginary frequency). Intrinsic reaction coordinate calculations[22,23] were used to ensure that the minima are connected by the appropriate transition structures.

A number of levels of theory were used to optimize geometries. These include the HF, MP2, and QCISD ab initio methods and the B3-LYP, MPW1K, and BMK density functional theory methods, using a range of basis sets. BMK is a hybrid functional that has been recently formulated by Boese and Martin.[24] We found that, for some of the alkoxy radicals, the lowest-energy conformer varies between optimization levels. To resolve these discrepancies, URCCSD-(T) single-point calculations were carried out on the structures optimized at the various levels, with the lowest energy indicating a preferred structure.

A number of levels of theory were also used to determine the energy profiles for reactions A1−A4. These include simpler procedures such as HF, MP2, QCISD, MPW1K, BMK, and B3-LYP with a variety of basis sets. Energies at 0 K were obtained by incorporating zero-point vibrational energies (ZPVEs) using appropriate scale factors.[25] In cases for which a scale factor is not available, these were taken from a closely related method. Specifically, for HF and MP2 in association with the 6-311++G(3df,2p) and 6-31G(2df,p) basis sets, the corresponding scale factors from the 6-311G-(d,p) basis set were used. In the case of B3-LYP in association with the 6-311+G(3df,2p) and cc-pVTZ basis sets, the 6-31G(2df,p) scale factor[26] was used, and in the case of MPWIK/6-31+G(3df,2p), the MPWIK/6-31+G(d,p) scale factor[27] was used. For the QCISD/6-31G(d) energy profiles, we used scaled UB3-LYP/6-31G(d) ZPVEs.

We also examined the performance of simple methods in which the energies and geometries were determined at separate levels of theory. These include UB3-LYP/6-311+G-(3df,2p)//UB3-LYP/6-31G(d), RB3-LYP/6-311+G(3df,2p)//UB3-LYP/6-31G(d), UBMK/6-311+G(3df,2p)//UB3-LYP/6-31G(d), RBMK/6-311+G(3df,2p)//UB3-LYP/6-31G(d), UBMK/6-311+G(3df,2p)//UBMK/6-31G(d), RBMK/6-311+G(3df,2p)//UBMK/6-31G(d), UMP2/6-311+G(3df,2p)//UB3-LYP/6-31G(d), and RMP2/6-311+G(3df,2p)//UB3-LYP/6-31G(d), corrected in each case with either scaled UB3-LYP/6-31G(d) ZPVEs or unscaled UBMK/6-31G(d) ZPVEs where appropriate.

Table 1. Calculated Differences in Energy (kJ mol^{-1}) between Conformers for the Alkoxy Radicals **a2** and **a4**[a]

level of theory	$\mathbf{a2_a} - \mathbf{a2_b}$	$\mathbf{a4_a} - \mathbf{a4_b}$	$\mathbf{a4_a} - \mathbf{a4_c}$
HF/6-31G(d)	−0.7	−0.4	9.6
HF/6-311++G(3df,2p)	0.6	0.8	9.5
MP2/6-31G(d)	−0.9	−1.1	4.9
MP2/6-31+G(d)	−1.0		
MP2/6-31+G(2df,p)	2.4		
B3-LYP/6-31G(d)	−3.0	−2.1	−10.2
B3-LYP/6-311+G(3df,2p)	−3.0	−1.4	−12.6
//HF/6-31G(d)	−0.4[b]	2.1[c]	1.5[c]
//MP2/6-31+G(2df,p)	0.9[b]		
//B3-LYP/6-31G(d)	0.6[b]	−0.7[c]	−5.2[c]
//B3-LYP/6-311+G(3df,2p)	−0.7[b]	−1.3[c]	−8.2[c]

[a] Energy differences are not corrected for zero-point vibrational energy. Geometries optimized at the same level as the energy calculations unless otherwise noted. [b] URCCSD(T)/6-311+G(3df,2p) calculations on the indicated geometry. [c] URCCSD(T)/6-311+G(d,p) calculations on the indicated geometry.

Finally, we used high-level composite methods such as CBS-QB3[28] and U-CBS-QB3[29] from the CBS family of methods, G3(MP2)//B3-LYP,[21] G3X(MP2)-RAD,[30] G3-RAD,[30] and G3//B3-LYP[21] from the G3 group of methods, and also the W1 method of Martin et al.[31] The performance and cost of CBS-QB3 is similar to that of CBS-RAD, which has previously been used to examine the cleavage of alkoxy radicals.[8]

3. Results and Discussion

3.1. Determination of Preferred Conformations. Our initial task was to determine the preferred conformations of the alkoxy radicals, the cleavage products, and the transition structures connecting reactants to products in each of the reactions A1−A4. These were initially screened with geometry optimizations at the B3-LYP/6-31G(d) level of theory. Further optimizations were carried out with B3-LYP and the larger 6-311+G(3df,2p) basis set and with the HF and MP2 methods in conjunction with the small and large basis sets. To examine the sensitivity of the relative energies of alternative possible conformations to the level of geometry optimization, single-point URCCSD(T) calculations were carried out on the various structures. The calculated relative energies are presented in Table 1. Based on the results of this analysis, discussed in more detail below, preferred structures for the alkoxy radicals (Figure 1, **a1**−**a4**), fragmentation products (Figure 2, **fp1**−**fp5**), and fragmentation (addition) transition structures (Figure 3, **ts1**−**ts4**) were identified. Figures 1−3 also include some of the more interesting structural parameters obtained at the B3-LYP/6-311+G(3df,2p) level of theory. Full structural data for equilibrium and transition structures are presented in the Supporting Information in the form of GAUSSIAN archive entries[17,18] for B3-LYP/6-311+G(3df,2p) optimized structures.

We begin our discussion by noting that acetaldehyde (CH_3-CH═O) is well known to have three equivalent conformational minima. Each of these conformers has a C−H bond eclipsing the C═O bond. If one of the methyl hydrogens of acetaldehyde is formally replaced by oxygen to give the

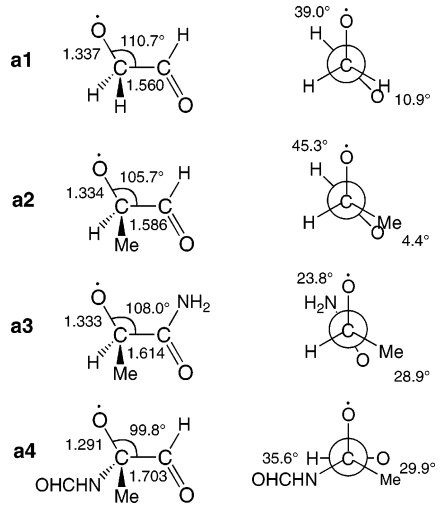

Figure 1. Optimized B3-LYP/6-311+G(3df,2p) structures of preferred conformers of the alkoxy radicals **a1**−**a4**.

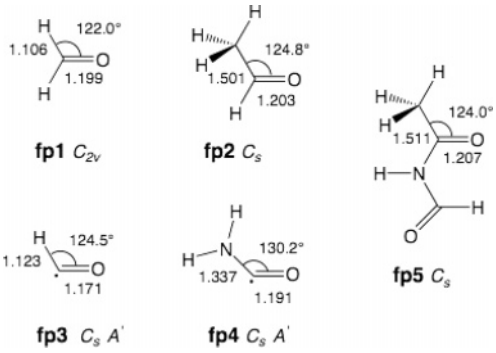

Figure 2. Optimized B3-LYP/6-311+G(3df,2p) structures of preferred conformers of the fragmentation products **fp1**−**fp5** of reactions A1−A4.

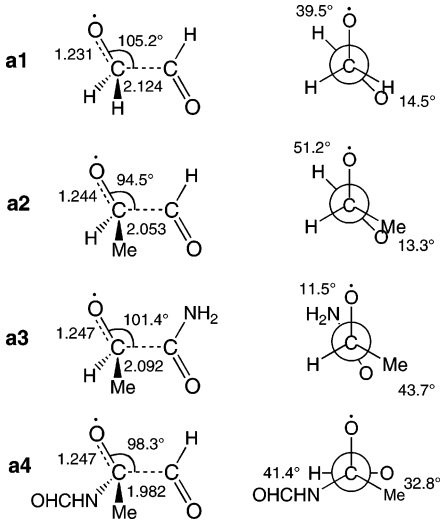

Figure 3. Optimized B3-LYP/6-311+G(3df,2p) transition structures for fragmentation of the C−C bond in reactions A1−A4.

•OCH_2CH═O radical (**a1**), we obtain the rotational potential of Figure 4. It can be seen that with HF/6-31G(d), the rotational potential around the central C−C bond changes from one with three equivalent conformers to one with just two distinct conformers. The preferred conformer has C_s

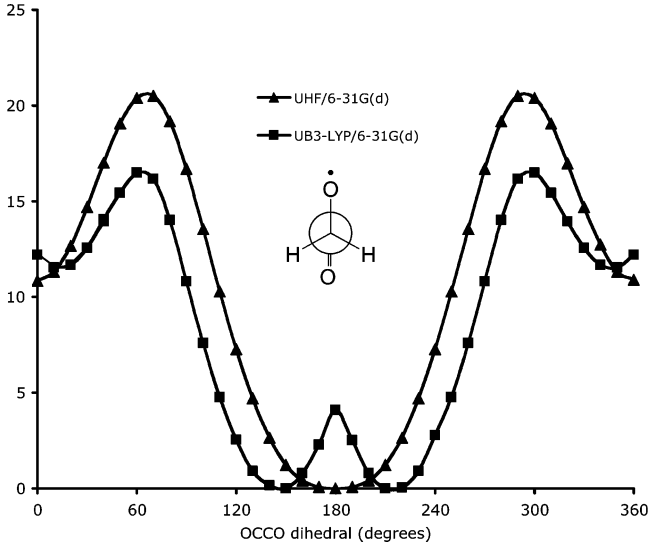

Figure 4. Rotational potential about the central C−C bond of the O═CH−$CH_2O^{\bullet}$ radical (**a1**) with HF/6-31G(d) and B3-LYP/6-31G(d).

symmetry (A″ state) with the oxygen atoms in an anti relationship. The other conformer, which is approximately 12.5 kJ mol^{-1} higher in energy after inclusion of ZPVE, is also C_s symmetric (A″ state) but with the oxygen atoms in a syn relationship. This behavior bears a qualitative similarity to the rotational potential of 2-fluoroacetaldehyde. [32]

At the B3-LYP/6-31G(d) level, there is a distortion from the syn and anti structures. In total, four stable conformers are found, a pair of enantiomeric C_1 structures that have OCCO dihedral angles of 145.6 and 214.4° (C−O• bond approximately anti to the C═O bond), respectively, and another enantiomeric pair that are 10 kJ mol^{-1} higher in energy, with dihedral angels of 13.3 and 346.7° (C−O• bond approximately syn to the C═O bond). Improving the basis set in the B3-LYP calculations to 6-311+G(3df,2p) has a relatively small effect on the rotational potential.

The B3-LYP rotational potential of Figure 4 suggests that alkoxy radical **a1** suffers from second-order Jahn−Teller (SOJT) effects.[33] It has been noted[33c] that density functional theory and coupled-cluster theory can reliably treat SOJT effects, while Hartree−Fock and MP theory do not. In the context of the present study, because of the possibility of SOJT effects, caution will be exercised when considering vibrational frequencies. We find that the energy differences between conformers that are distorted through SOJT effects are quite small. For example, at the B3-LYP/6-31G(d) level, the difference in energy between the constrained C_s (A″ state) conformer with C−O• anti to C═O (which has one imaginary frequency) and the energetically lower C_1 structure (no imaginary frequencies) is just 1.7 kJ mol^{-1}.

The $^{\bullet}OCH(CH_3)CH{=}O$ radical (**a2**) is obtained formally by replacing one of the oxy-carbon hydrogens of **a1** with a methyl group. The possible symmetric structures obtained with HF/6-31G(d) for **a1** cannot be achieved by alkoxy radical **a2**. At this level, three conformers are found for **a2** with OCCO dihedral angles of 5.3° (C−O• bond approximately eclipsing C═O bond), 166.2° (a distortion of the structure with the C−O• bond anti to C═O), and 202.3° (a distortion in the opposite direction of the structure with the C−O• bond anti to C═O), which can be interpreted as a modification of the fluoroacetaldehyde rotational potential.

The conformers with OCCO dihedral angles of 166.2° (**a2**$_a$) and 202.3° (**a2**$_b$) at HF/6-31G(d) were reoptimized at a number of levels of theory. URCCSD(T)/6-311+G-(3df,2p) single points were then carried out on a selection of the optimized geometries.

The results in Table 1 show that the preferred conformer depends on the level of theory, but the energy differences are small. We have taken our best level for geometry optimization throughout this study to be B3-LYP/6-311+G-(3df,2p), and the conformation that gives the lowest coupled-cluster energy at this level was therefore taken to be the preferred structure. For $^{\bullet}OCH(CH_3)CH{=}O$, **a2**$_a$ is thus our predicted structure. At the B3-LYP/6-311+G(3df,2p) level, the OCCO dihedral angle in **a2**$_a$ is 134.2°.

For $^{\bullet}OCH(CH_3)C(NH_2){=}O$ (**a3**), analogies with fluoroacetaldehyde are not apparent. In this case, only one conformation of significance was found (Figure 1), and so no further analysis was carried out.

For the $^{\bullet}OC(CH_3)(NHCH{=}O)CH{=}O$ radical (**a4**), three conformers were examined in detail, namely **a4**$_a$, which has the C═O bond approximately eclipsing the C−CH_3 bond, and **a4**$_b$ and **a4**$_c$, both of which have the C═O bond approximately eclipsing the C−N bond but which differ in the orientation of the NHCH═O group. The detailed geometries for each conformer at the B3-LYP/6-311+G-(3df,2p) level can be found in the Supporting Information. The energetic ordering at various levels of theory of the three conformers are summarized in Table 1. The conformer that gives the lowest coupled-cluster energy for the B3-LYP/6-311+G(3df,2p) geometry is conformer **a4**$_a$, shown as **a4** in Figure 1, and so this was used in the subsequent calculations.

The geometries of fragmentation products were also obtained by initially scanning for the lowest-energy conformations. Unlike the situation for the alkoxy radicals, there was general agreement as to the preferred conformations at the various levels of theory. These are displayed in Figure 2.

Transition structures were found by initially determining single-point energy profiles at the B3-LYP/6-31G(d) level as the cleaving bond was stretched, starting with the preferred conformers of the alkoxy radicals. This procedure identified approximate transition structures, which were refined by full geometry optimizations. Using IRC calculations, we confirmed that the transition structures were connected to the initial alkoxy radicals. However, these transition structures do not necessarily connect directly to the global conformational minima of the products. It is assumed that the energy required for the products to subsequently rearrange to the preferred conformer through torsional motions is small compared with the energy required for the initial bond cleavage.

In summary, assignment of the preferred conformations for the alkoxy radicals **a2**−**a4** is sensitive to the level of theory used for geometry optimization. We have taken the preferred conformation to be the one that gives the lowest CCSD(T) energy with B3-LYP/6-311+G(3df,2p) geometries.

Table 2. Effect of Geometry on Calculated Enthalpy for Reaction A1 and on Cleavage and Addition Barriers (UCCSD(T)6-311+G(3df,2p), kJ mol^{-1})[a]

geometry	ΔH	$\Delta H^{\ddagger}_{cleavage}$	$\Delta H^{\ddagger}_{addition}$
//UHF/6-31G(d)	20.3	42.4	22.1
//UMP2/6-31G(d)	19.4	42.0	22.6
//UMPW1K/6-31+G(d,p)	20.1	40.5	20.4
//UMPW1K/6-31+G(3df,2p)	21.0	41.2	20.2
//UBMK/6-31G(d)	19.6	40.6	20.9
//UB3-LYP/6-31G(d)	19.7	41.5	21.8
//UB3-LYP/6-31G(2df,p)	18.3	40.4	22.1
//UB3-LYP/6-311+G(3df,2p)	18.3	40.5	22.2
//UB3-LYP/cc-pVTZ	18.6	40.9	22.3
//UQCISD/6-31G(d)	20.1	43.8	23.7

[a] Enthalpies and barriers are not corrected for zero-point vibrational energy.

Table 3. Effect of Geometry on Calculated Enthalpy for Reaction A2 and on Cleavage and Addition Barriers (URCCSD(T)6-311+G(d,p), kJ mol^{-1})[a]

geometry	ΔH	$\Delta H^{\ddagger}_{cleavage}$	$\Delta H^{\ddagger}_{addition}$
//UHF/6-31G(d)	1.7	32.7	31.0
//UHF/6-311++G(3df,2p)	5.8	34.0	28.2
//UMP2/6-31G(d)	0.6	37.1	36.5
//UMP2/6-31+G(d)	1.0	36.4	35.4
//UMP2/6-31+G(2df,p)	1.2	39.8	38.6
//UBMK/6-31G(d)	−0.2	33.2	33.5
//UB3-LYP/6-31G(d)	−0.2	33.5	33.7
//UB3-LYP/6-31G(2df,p)	−1.7	32.4	34.1
//UB3-LYP/6-311+G(3df,2p)	−2.5	32.4	34.9

[a] Enthalpies and barriers are not corrected for zero-point vibrational energy.

The theoretical determination of the preferred geometries of the transition structures and products is found to be more straightforward than for the alkoxy radical reactants.

3.2. Effect of Level of Geometry Optimization on Calculated Reaction Enthalpies and Barriers. Having selected the preferred conformations of each of the alkoxy radicals, cleavage products (addition reactants), and transition structures, we next sought to determine the sensitivity of the calculated reaction enthalpies and barriers to the level of geometry optimization. To do this, we calculated the enthalpies and barriers for reactions A1−A3 by obtaining CCSD(T) energies for a variety of optimized structures. For reaction A1, calculations were carried out with UCCSD(T)/6-311+G(3df,2p). For reactions A2 and A3, calculations were carried out with URCCSD(T)/6-311+G(d,p) or URCCSD(T)/6-311+G(2df,p). The results of this analysis are summarized in Tables 2−4.

Table 2 shows that the reaction enthalpies and barriers for reaction A1 are not very sensitive to the method used to optimize the structures. In this case, the enthalpies and barriers all agree to within 3.5 kJ mol^{-1}. The enthalpies and barriers for reactions A2 and A3 are somewhat more sensitive to the level of geometry optimization, although for the most part the effects are still not very large. The greater sensitivity may in part be due to the reduced basis set size. It is noteworthy that the basis set effects appear smaller for B3-LYP than for HF or MP2.

Table 4. Effect of Geometry on Enthalpies for Reaction A3 and on Cleavage and Addition Barriers (URCCSD(T)6-311+G(2df,p), kJ mol^{-1})[a]

geometry	ΔH	$\Delta H^{\ddagger}_{cleavage}$	$\Delta H^{\ddagger}_{addition}$
//UHF/6-31G(d)	−17.7	5.5	23.3
//UHF/6-311++G(3df,2p)	−28.3	3.5	31.8
//UMP2/6-31+G(d)	−25.2	2.7	27.8
//UB3-LYP/6-31G(d)	−20.8	5.4	26.2
//UB3-LYP/6-31G(2df,p)	−19.7	6.3	26.0
//UB3-LYP/6-311+G(3df,2p)	−19.3	6.8	26.1

[a] Enthalpies and barriers are not corrected for zero-point vibrational energy.

Table 5. Calculated Lengths of Cleaving (Forming) Bonds (Å) in Transition Structures for Reactions A1−A4

level of theory	**ts1**	**ts2**	**ts3**	**ts4**
HF/6-31G(d)	2.078	2.052	2.044	1.975
HF/6-311++G(3df,2p)	2.046	2.020	2.015	
MP2/6-31G(d)	1.961	1.926	1.884	1.801
MP2/6-31+G(d)	1.954	1.917	1.875	
MP2/6-311+G(3df,2p)	1.930			
MPW1K/6-31+G(d,p)	2.174	2.096	2.159	
MPW1K/6-31+G(3df,2p)	2.170			
BMK/6-31G(d)	2.138	2.071	2.165	2.047
B3-LYP/6-31G(d)	2.148	2.068	2.155	2.024
B3-LYP/6-31G(2df,p)	2.103	2.045	2.125	1.998
B3-LYP/6-311+G(3df,2p)	2.124	2.040	2.092	1.981
QCISD/6-31G(d)	2.025			

Table 5 lists the lengths of the fragmenting (forming) bonds in the cleavage (addition) transition structures of reactions A1−A4, as calculated at a variety of theoretical levels. It can be seen that the B3-LYP and MPW1K DFT methods tend to predict longer bonds than the corresponding HF and MP2 bonds, consistent with previous observations.[34] The BMK functional predicts bond lengths similar to those of the other DFT methods, despite its formulation as a functional to give improved kinetic parameters.

In summary, assessment of the effect of geometry on the calculated reaction enthalpies and barriers indicates that the level of theory used for geometry optimization does not have a great effect on these properties. This lends confidence to the use of B3-LYP geometries in calculating improved energies with composite methods.

3.3. Assessment of Reaction Energies and Barriers. Enthalpies and barriers for reactions A1−A4, and barriers for the reverse addition reactions at various levels of theory, are given in Tables 6−9. In this section, we initially describe the results obtained with high-level composite methods. We then examine the results from several computationally more efficient levels that are more amenable to application to larger systems and gauge their performance against that of the high-level methods. All of the high-level composite methods we use prescribe B3-LYP geometries. We found in the previous section that this should not have a large effect on the calculated relative energies.

The highest-level method used in the present study is W1, which was restricted to the calculation of the addition barrier for reaction A1. The highest-level method used for all four

Table 6. Effect of Level of Theory on Calculated Enthalpy of Reaction A1 and on Barriers for Fragmentation and Addition (0 K, kJ mol^{-1})

level of theory	ΔH	$\Delta H^{\ddagger}_{\text{cleavage}}$	$\Delta H^{\ddagger}_{\text{addition}}$
W1			26.6
G3//B3-LYP	2.9	27.5	24.6
G3-RAD	4.2	30.4	26.1
CBS-QB3	3.1	24.4	21.2
U-CBS-QB3	3.2	27.9	24.7
G3X(MP2)-RAD	0.4	29.4	29.0
G3(MP2)//B3-LYP	0.5	26.1	25.7
UB3-LYP/6-311+G(3df,2p)//B3[a]	5.4	23.7	18.2
RB3-LYP/6-311+G(3df,2p)//B3[a]	9.6	23.7	14.1
UBMK/6-311+G(3df,2p)//B3[a]	13.1	35.9	22.7
RBMK/6-311+G(3df,2p)//B3[a]	11.8	37.8	26.0
UBMK/6-311+G(3df,2p)//BM[b]	13.1	36.5	23.3
RBMK/6-311+G(3df,2p)//BM[b]	9.8	36.5	26.5
UMP2/6-311+G(3df,2p)//B3[a]	−23.8	38.9	62.7
RMP2/6-311+G(3df,2p)//B3[a]	−26.9	−0.6	26.3
UQCISD/6-31G(d)	12.5	53.9	41.4
UB3-LYP/cc-pVTZ	10.8	29.0	18.2
UB3-LYP/6-311+G(3df,2p)	9.7	28.3	18.6
UB3-LYP/6-31G(2df,p)	17.0	30.7	13.8
UB3-LYP/6-31G(d)	24.8	36.7	12.0
UMPW1K/6-31+G(3df,2p)	46.2	61.0	14.8
UMPW1K/6-31+G(d,p)	54.9	70.3	15.4
UMP2/6-311+G(3df,2p)	−21.9	46.4	68.3
UMP2/6-31G(2df,p)	−13.7	53.2	66.8
UMP2/6-31G(d)	−5.9	75.1	81.0
UHF/6-311++G(3df,2p)	38.6	96.5	58.0
UHF/6-31G(d)	60.1	107.8	47.7

[a] The notation//B3 is used to designate that the calculations were carried out on UB3-LYP/6-31G(d) optimized structures. [b] The notation//BM is used to designate that the calculations were carried out on UBMK/6-31G(d) optimized structures.

Table 7. Effect of Level of Theory on Calculated Enthalpy of Reaction A2 and on Barriers for Fragmentation and Addition (0 K, kJ mol^{-1})

level of theory	ΔH	$\Delta H^{\ddagger}_{\text{cleavage}}$	$\Delta H^{\ddagger}_{\text{addition}}$
G3//B3-LYP	−12.3	21.1	33.4
G3-RAD	−12.7	21.6	34.3
CBS-QB3	−10.8	19.2	30.0
U-CBS-QB3	−10.7	22.6	33.3
G3X(MP2)-RAD	−13.6	23.5	37.1
G3(MP2)//B3-LYP	−14.5	19.9	34.4
UB3-LYP/6-311+G(3df,2p)//B3[a]	−14.1	20.4	34.5
RB3-LYP/6-311+G(3df,2p)//B3[a]	−16.2	19.7	35.9
UBMK/6-311+G(3df,2p)//B3[a]	−7.2	28.9	36.1
RBMK/6-311+G(3df,2p)//B3[a]	−8.5	30.2	38.7
UBMK/6-311+G(3df,2p)//BM[b]	−6.9	29.3	36.2
RBMK/6-311+G(3df,2p)//BM[b]	−8.7	30.0	38.7
UMP2/6-311+G(3df,2p)//B3[a]	−42.4	27.5	69.9
RMP2/6-311+G(3df,2p)//B3[a]	−45.7	−13.0	32.7
UB3-LYP/6-311+G(3df,2p)	−13.9	19.3	35.0
UB3-LYP/6-31G(2df,p)	−2.9	23.9	28.7
UB3-LYP/6-31G(d)	4.0	28.7	26.7
UMP2/6-31+G(2df,p)	−37.9	33.8	71.8
UMP2/6-31+G(d)	−53.5	29.6	85.3
UMP2/6-31G(d)	−30.3	51.6	84.1
UHF/6-31G(d)	34.2	97.5	63.4
UHF/6-311++G(3df,2p)	12.2	87.5	75.3

[a] The notation//B3 is used to designate that the calculations were carried out on UB3-LYP/6-31G(d) optimized structures. [b] The notation//BM is used to designate that the calculations were carried out on UBMK/6-31G(d) optimized structures.

Table 8. Effect of Level of Theory on Calculated Enthalpy of Reaction A3 and on Barriers for Fragmentation and Addition (0 K, kJ mol^{-1})

level of theory	ΔH	$\Delta H^{\ddagger}_{\text{cleavage}}$	$\Delta H^{\ddagger}_{\text{addition}}$
G3//B3-LYP	12.7	14.1	1.4
CBS-QB3	15.1	13.9	−1.2
U-CBS-QB3	15.1	16.5	1.4
G3X(MP2)-RAD	13.4	19.1	5.6
G3(MP2)//B3-LYP	10.8	13.5	2.7
UB3-LYP/6-311+G(3df,2p)//B3[a]	5.1	14.4	9.3
RB3-LYP/6-311+G(3df,2p)//B3[a]	3.1	14.1	11.0
UBMK/6-311+G(3df,2p)//B3[a]	16.4	23.8	7.5
RBMK/6-311+G(3df,2p)//B3[a]	14.2	24.4	10.2
UBMK/6-311+G(3df,2p)//BM[b]	15.4	22.7	7.4
RBMK/6-311+G(3df,2p)//BM[b]	9.4	19.6	10.2
UMP2/6-311+G(3df,2p)//B3[a]	−16.0	8.9	24.9
RMP2/6-311+G(3df,2p)//B3[a]	−19.4	−18.6	0.8
UB3-LYP/6-311+G(3df,2p)	2.0	11.6	9.6
UB3-LYP/6-31G(2df,p)	21.8	18.2	−3.6
UB3-LYP/6-31G(d)	26.8	23.2	−3.5
UMP2/6-31+G(d)	−5.7	41.3	47.0
UMP2/6-31G(d)	−2.0	38.6	40.6
UHF/6-311++G(3df,2p)	33.4	89.8	56.4
UHF/6-31G(d)	52.3	96.5	44.2

[a] The notation//B3 is used to designate that the calculations were carried out on UB3-LYP/6-31G(d) optimized structures. [b] The notation//BM is used to designate that the calculations were carried out on UBMK/6-31G(d) optimized structures.

reactions is G3//B3-LYP. We will use this procedure to compare the performance of the other methods. Other high-level methods used for all four reactions are standard CBS-QB3, U-CBS-QB3, G3(MP2)//B3-LYP, and G3X(MP2)-RAD. Mean absolute deviations (MADs) from G3//B3-LYP for all enthalpies and barriers (cleavage and addition) are 2.2 (CBS-QB3), 1.3 (U-CBS-QB3), 1.5 (G3(MP2)//B3-LYP), and 2.8 (G3X(MP2)-RAD) kJ mol^{-1}. The MADs show that the high-level procedures agree well with one another, although it can be argued that a sample size of 12 may not be statistically significant. G3(MP2)//B3-LYP and G3X(MP2)-RAD are considerably cheaper than the other methods but give comparable performance.

The standard G*n* methods are less reliable when open-shell species have large spin contamination in the unrestricted wave functions. The RAD variants of the G*n* methods[30] were designed specifically to alleviate this situation. In the present study, we used G3-RAD to calculate enthalpies and barriers for reactions A1 and A2 (Tables 6 and 7) and G3X(MP2)-RAD (Tables 6−9) to calculate enthalpies and barriers for reactions A1−A4.

G3-RAD produces enthalpies and barriers that are similar to those from the G3//B3-LYP method. For the enthalpies of reactions A1 and A2, this is not unexpected. The spin contamination of the alkoxy radicals and the product radicals formed in the cleavage reactions is very small. At the UMP2/6-31G(d) level, the $\langle S^2 \rangle$ values are less than 0.77, compared with 0.75 for a pure doublet. The transition structures for

Table 9. Effect of Level of Theory on Calculated Enthalpy of Reaction A4 and on Barriers for Fragmentation and Addition (0 K, kJ mol^{-1})

level of theory	ΔH	$\Delta H^{\ddagger}_{cleavage}$	$\Delta H^{\ddagger}_{addition}$
G3//B3-LYP	−49.8	−4.6	45.2
CBS-QB3	−45.8	−4.2	41.6
U-CBS-QB3	−46.3	−2.2	44.1
G3X(MP2)-RAD	−51.9	−2.9	49.1
G3(MP2)//B3-LYP	−52.2	−5.8	46.3
UB3-LYP/6-311+G(3df,2p)//B3[a]	−60.8	−1.1	59.7
RB3-LYP/6-311+G(3df,2p)//B3[a]	−62.9	−2.1	60.8
UBMK/6-311+G(3df,2p)//B3[a]	−54.3	4.6	58.9
RBMK/6-311+G(3df,2p)//B3[a]	−57.7	3.8	61.4
UBMK/6-311+G(3df,2p)//BM[b]	−55.7	1.8	57.6
RBMK/6-311+G(3df,2p)//BM[b]	−60.2	0.0	60.2
UMP2/6-311+G(3df,2p)//B3[a]	−91.5	−18.8	72.7
RMP2/6-311+G(3df,2p)//B3[a]	−98.0	−55.2	42.8
UB3-LYP/6-311+G(3df,2p)	−60.5	0.4	60.8
UB3-LYP/6-31G(2df,p)	−49.1	2.8	51.9
UB3-LYP/6-31G(d)	−44.4	6.0	50.3
UMP2/6-31G(d)	−83.4	9.0	92.5
UHF/6-31G(d)	−43.4	66.7	110.1

[a] The notation//B3 is used to designate that the calculations were carried out on UB3-LYP/6-31G(d) optimized structures. [b] The notation//BM is used to designate that the calculations were carried out on UBMK/6-31G(d) optimized structures.

reactions A1 and A2 have larger $\langle S^2 \rangle$ values (0.89 and 0.88, respectively), and so it is more surprising that the difference between G3-RAD and G3//B3-LYP barriers for these two reactions is small. With G3X(MP2)-RAD, enthalpies and barriers for reactions A1 and A2 as well as for A3 and A4 compare well with G3//B3-LYP. This is characterized by the relatively small MAD of 2.8 kJ mol^{-1}, as quoted above.

Enthalpies and barriers calculated from UB3-LYP/6-311+G(3df,2p)//UB3-LYP/6-31G(d) and RB3-LYP/6-311+G(3df,2p)//UB3-LYP/6-31G(d) energies give fairly good agreement with those of the high-level methods. MADs from the G3//B3-LYP results are 5.1 and 5.6 kJ mol^{-1}, and the largest deviations (LDs) are 15.6 and 14.5 kJ mol^{-1} for UB3-LYP/6-311+G(3df,2p)//UB3-LYP/6-31G(d) and RB3-LYP/6-311+G(3df,2p)//UB3-LYP/6-31G(d), respectively. The relatively small MADs and LDs make these methods candidates for use with larger systems when G3(MP2)//B3-LYP and G3X(MP2)-RAD become too costly. The very small difference between the two methods is not surprising when considering the $\langle S^2 \rangle$ values for the alkoxy radicals, product radicals, and transition structures. For UB3-LYP/6-311+G(3df,2p)//UB3-LYP/6-31G(d), $\langle S^2 \rangle$ values are always less than 0.76.

We note that the UB3-LYP/6-311+G(3df,2p) enthalpies and barriers obtained from fully optimized UB3-LYP/6-311+G(3df,2p) structures are close to those obtained from UB3-LYP/6-311+G(3df,2p)//UB3-LYP/6-31G(d). The MAD for the fully optimized UB3-LYP/6-311+G(3df,2p) structures increases slightly to 5.9 kJ mol^{-1} and has an LD of 15.6 kJ mol^{-1}. B3-LYP enthalpies and barriers obtained with smaller basis sets, viz. 6-31G(d) and 6-31G(2df,p), are somewhat poorer. Thus, for B3-LYP/6-31G(d), the MAD and LD are 10.8 and 21.9 kJ mol^{-1}, while for B3-LYP/6-31G(2df,p) they are 6.4 and 14.1 kJ mol^{-1}, respectively.

The MADs of 6.9 and 7.6 kJ mol^{-1} for UBMK/6-311+G(3df,2p)//UB3-LYP/6-31G(d) and RBMK/6-311+G(3df,2p)//UB3-LYP/6-31G(d), respectively, demonstrate that these two methods, like the analogous B3-LYP calculations, are also potentially cost-effective alternatives to the more sophisticated composite methods. The MADs are improved to 6.5 kJ mol^{-1} for UBMK/6-311+G(3df,2p) and to 6.9 kJ mol^{-1} for RBMK/6-311+G(3df,2p) if UBMK/6-31G(d) geometries are used in place of the UB3LYP/6-31G(d) geometries.

Enthalpies and barriers calculated with HF and MP2 in general are not very satisfactory. The MADs for UMP2/6-311+G(3df,2p)//UB3-LYP/6-31G(d) and RMP2/6-311+G(3df,2p)//UB3-LYP/6-31G(d) are 24.1 and 23.7 kJ mol^{-1}, with LDs of 41.7 and 48.2 kJ mol^{-1}, respectively. For UMP2/6-311+G(3df,2p)//UB3-LYP/6-31G(d), it is interesting that the addition barriers agree reasonably well with G3//B3-LYP with an LD of 14.2 kJ mol^{-1}, while the cleavage barriers are poor with an LD of 38.0 kJ mol^{-1}. On the other hand, the addition barriers are poor with RMP2/6-311+G(3df,2p)//UB3-LYP/6-31G(d) with an LD of 50.7 kJ mol^{-1}, but the cleavage barriers are good with an LD of 2.4 kJ mol^{-1}. For both UMP2/6-311+G(3df,2p)//UB3-LYP/6-31G(d) and RMP2/6-311+G(3df,2p)//UB3-LYP/6-31G(d), the reaction enthalpies are similar and consistently too exothermic.

The differences between the RMP2 and UMP2 results can be rationalized in terms of the general performance of MP2 theory in describing alkoxy radicals and the $\langle S^2 \rangle$ values of the alkoxy radicals and the transition structures. As noted in the section on conformers, MP2 theory predicts higher than expected energies for the alkoxy radicals. However, MP2 theory performs reasonably in the calculation of the fragmentation products. This leads to a greater than expected calculated exothermicity. The UMP2 and RMP2 reaction enthalpies are similar because of low spin contamination in both the alkoxy radicals and their associated products, i.e., the errors in the enthalpies are associated with MP2 rather than spin contamination. Large spin contamination becomes a problem in the transition structures at the UMP2 level. UMP2/6-31G(d) $\langle S^2 \rangle$ values for the transition structures of reactions A1−A4 are 0.89, 0.87, 0.84, and 0.81, respectively. This leads to a fortuitous cancellation of errors when calculating fragmentation barriers with UMP2, but poor fragmentation barriers with RMP2. For the same reasons, addition barriers are poor at the UMP2 level but good with RMP2.

Additional UMP2 and UHF enthalpies and barriers were calculated from optimizations at these levels using a variety of basis sets. These include 6-31G(d), 6-31+G(d), 6-31G(2df,p), 6-31+G(2df,p), 6-31+G(3df,2p), and 6-311++G(3df,2p). As expected from the discussion above, enthalpies and addition barriers are poor with no substantial improvement with basis set size.

The remaining methods that were examined involve full geometry optimizations at the UMPW1K and UQCISD levels of theory with various basis sets for reaction A1. The results are summarized in Table 6. For UMPW1K with small and large basis sets, the deviations from the G3//B3-LYP results are large. UQCISD/6-31G(d) also does not perform well in

Table 10. Effect of Level of Theory on Calculated Heats of Formation (0 K, kJ mol^{-1}) of Fragmentation Products (**fp1**−**fp5**) and of Alkoxy Radicals (**a1**−**a4**)[a]

level of theory	fp1	fp2	fp3	fp4	fp5	a1	a2	a3	a4
B3-LYP/6-311+G(3df,2p)//B3	−107.2	−152.4	31.3	−36.4	−351.8	−81.4	−101.5	−193.9	−259.8
B3-LYP/6-311+G(3df,2p)	−108.4	−154.6	30.3	−37.2	−355.3	−87.9	−109.9	−192.7	−264.6
CBS-QB3	−109.1	−155.7	41.3	−7.6	−354.9	−70.9	−102.1	−178.3	−267.7
U-CBS-QB3	−110.9	−158.1	39.9	−8.9	−359.0	−74.2	−106.1	−182.1	−272.8
G3(MP2)//B3-LYP	−108.9	−156.3	37.4	−5.5	−349.5	−71.9	−101.4	−172.6	−259.9
G3X(MP2)-RAD	−108.3	−155.8	40.1[f]	−3.2	−349.1	−68.6	−100.3	−172.5	−257.1
G3//B3-LYP	−108.7	−157.0	39.1	−7.5	−354.1	−72.6	−102.7	−177.2	−265.3
G3-RAD(6d,10f)	−107.4	−156.2	41.0[f]	−2.8	−350.2	−70.7	−102.6		
W1	−107.3		40.5						
expt	−104.6 ± 0.7[b]	−155.0[b]	41.3 ± 0.8[c]/ 44.6 ± 0.4[d,e]						

[a] See Figures 1 and 2 for B3-LYP/6-311+G(3df,2p) structures of **a1**−**a4** and **fp1**−**fp5**, respectively. [b] From ref . 39. [c] From ref 43. [d] From ref 42. [e] $\Delta_f H_{298}$ back-corrected to 0 K using theoretical temperature correction from B3-LYP/6-31G(d) frequencies (scaled by 0.9989[25]): see ref 41. [f] From ref 41.

comparison with the high-level methods. Contributing factors to this result are most probably the small basis set and the omission of the perturbative triples.

In summary, high-level composite methods are in generally good agreement with one another for the reaction enthalpies and barriers (both cleavage and addition). The best composite methods in terms of accuracy and cost are G3(MP2)//B3-LYP and G3X(MP2)-RAD, which give enthalpies and barriers in good agreement with the more expensive G3//B3-LYP, G3-RAD, CBS-QB3, and U-CBS-QB3 methods. Relatively accurate but low-cost methods suitable for application to larger systems are provided by single-point energy calculations with UB3-LYP/6-311+G(3df,2p), RB3-LYP/6-311+G(3df,2p), UBMK/6-311+G(3df,2p), or RBMK/6-311+G(3df,2p) on UB3-LYP/6-31G(d) geometries. Using UBMK/6-31G(d) geometries in place of UB3-LYP/6-31G(d) geometries has only a small effect. UMP2/6-311+G(3df,2p)//UB3-LYP/6-31G(d) calculations appear to give good results for the cleavage barriers but not for addition barriers. On the other hand RMP2/6-311+G(3df,2p)//UB3-LYP/6-31G(d) calculations appear to give good results for the addition barriers but not for cleavage barriers. Neither of these two methods is suitable for the calculation of the reaction enthalpies.

3.4. Heats of Formation. Heats of formation at 0 K for the fragmentation products (**fp1**−**fp5**) and the four substituted alkoxyl radicals (**a1**−**a4**) of reactions A1−A4 were calculated at various levels of theory. These results are compared with available experimental values in Table 10.

In general, the high-level methods agree well with one another and with available experimental data. B3-LYP gives varied results, with discrepancies of up to 30 kJ mol^{-1} in some cases, and only a few kJ mol^{-1} in others. It has previously been found that B3-LYP/6-311+G(3df,2p) enthalpies of formation for species in the G3/99 test set have an MAD from reliable experimental values of 22.6 kJ mol^{-1}.[35] The B3-LYP results of this section are better than expected on this basis since all but one of the enthalpies of formation have deviations less than this value. It has also previously been found that errors accumulate in the B3-LYP heats of formation as the size of the system increases. This is why the G3/99 test set, with an average of approximately 17 electron pairs per species, has a larger MAD (22.6 kJ mol^{-1}) for heats of formation compared with the G2/97 test set (13.7 kJ mol^{-1}), which has an average of approximately 11 electron pairs per species. We do not find such a correlation for the small number of species in the present study, indicating that other effects are having a more important influence in these cases. For example, the B3-LYP/6-311+G(3df,2p)//B3-LYP/6-31G(d) heat of formation of $^{\bullet}OC(CH_3)(NHCH{=}O)CH{=}O$ (**a4**), which has 22 electron pairs, deviates by 5.5 kJ mol^{-1} from the G3//B3-LYP value. On the other hand, the B3-LYP/6-311+G(3df,2p)//B3-LYP/6-31G(d) heat of formation of $NH_2(C^{\bullet}){=}O$ (**fp4**), which has 8 electron pairs, deviates by 28.9 kJ mol^{-1} from the G3//B3LYP value.

Surprisingly the heats of formation calculated with BMK/6-311+G(3df,2p)//B3-LYP/6-31G(d)[36] differ significantly from the corresponding B3-LYP/6-311+G(3df,2p) values, and this method therefore does not appear to be suitable for calculating heats of formation for the alkoxy radicals.

$CH_2{=}O$ (fp1). Formaldehyde is a well-studied molecule and is primarily included in Table 10 for the sake of completeness. Our high-level methods agree in their predicted heats of formation for formaldehyde to within 1.8 kJ mol^{-1}, with W1, the highest level used in this study, predicting a value of −107.3 kJ mol^{-1}. It is evident that both the current theoretical predictions and other recent high-level theoretical predictions, e.g. the W2 and W3 results of Martin,[37] are consistently more negative than the experimental heat of formation, −104.6 ± 0.7 kJ mol^{-1},[38] by about 3 kJ mol^{-1}. The reason for this apparent discrepancy is not clear.

$CH_3CH{=}O$ (fp2). Acetaldehyde, also has a well-characterized experimental heat of formation (−155.0 kJ mol^{-1}).[39] The high-level theoretical values are all in good agreement with this experimental value. The largest deviation from experiment is 3.1 kJ mol^{-1} at the U-CBS-QB3 level.

$^{\bullet}CH{=}O$ (fp3). The heat of formation of the formyl radical has been theoretically investigated in several high-level studies. Most recently, Feller et al.[40] have used various extrapolation schemes of coupled-cluster energies to obtain a value of 43.5 ± 0.8 kJ mol^{-1}. The associated error has been estimated from the spread of data given by the different extrapolations. Earlier, Henry et al.[41] used a number of high-

level composite methods to calculate $\Delta_f H°_0$(•CHO), obtaining values of 40.1 (G3X(MP2)-RAD) and 41.0 (G3-RAD-(6d,10f)) kJ mol^{-1} (Table 10). Two experimental values are available, the more recent value of 44.6 ± 0.4 coming from Becerra et al.[42] and an earlier value of 41.3 ± 0.8 kJ mol^{-1} from Berkowitz et al.[43] The W1, G3-RAD, and G3X(MP2)-RAD estimates all fall within the experimental uncertainty of the Berkowitz et al.[39] result. However, the theoretical value of Feller et al.[40] is in better agreement with the more recent result of Becerra et al.[42]

$NH_2C(•)=O$ (fp4). A heat of formation for the $NH_2C(•)=O$ fragmentation product of reaction A3 has not been reported in the literature. The heats of formation predicted by the high-level methods range between −3.2 kJ mol^{-1} from G3X(MP2)-RAD to −8.9 kJ mol^{-1} from U-CBS-QB3. The previous comparisons with experimental values suggest that U-CBS-QB3 might slightly underestimate heats of formation, and so this value may be too low. The B3-LYP values are more negative by 30 kJ mol^{-1} compared with those from the high-level composite methods. If we average the high-level methods, i.e., all the values in Table 10 except the B3-LYP estimates, we obtain −5.9 kJ mol^{-1} as the 0 K heat of formation for **fp4**.

$CH(=O)NHC(CH_3)=O$ (fp5). The previous observation that U-CBS-QB3 seems to underestimate heats of formation also applies in the case of **fp5**. Compared with the other high-level methods, U-CBS-QB3 gives the most negative heat of formation of −359.0 kJ mol^{-1}. In contrast to **fp4**, the B3-LYP values compare well with the remaining high-level methods. By averaging the results of all the high-level methods in Table 10, we obtain −352.8 kJ mol^{-1} for the 0 K heat of formation for $CH(=O)NHC(CH_3)=O$ (**fp5**).

Alkoxy Radicals (a1−a4). As in the case of the fragmentation products discussed in the preceding paragraphs, the high-level methods are in good agreement with one another. Another continued trend is the underestimation of the heats of formation by U-CBS-QB3. The B3-LYP methods give mixed results. In the case of **a1** and **a3**, the values are somewhat outside the ranges of the high-level methods. However, for alkoxy radicals **a2** and **a4** the B3-LYP heats of formation are in good agreement with the high-level results. If we average the values from the high-level methods in Table 10, we obtain heats of formation at 0 K for the alkoxy radicals of −71.4 (**a1**), −102.5 (**a2**), −176.6 (**a3**), and −264.6 (**a4**) kJ mol^{-1}, respectively.

In summary, heats of formation at 0 K calculated by high-level methods agree well with one another. U-CBS-QB3 seems to underestimate the heats of formation when compared with the other high levels of theory, but the deviation is only small. In recommending heats of formation, we average the high-level results (including U-CBS-QB3). Alkoxy radical **a4** gives the largest range of such values (10.4 kJ mol^{-1}), but for the other species, the range of values is much less (5.8 kJ mol^{-1}). B3-LYP gives varied results, with discrepancies of up to 30 kJ mol^{-1} in some cases, and only a few kJ mol^{-1} in others.

4. Concluding Remarks

The purpose of the present study has been to establish methodologies for investigating the C−C β-scission reactions of substituted alkoxy radicals that might serve as models for peptide backbone alkoxy radicals. We seek methods that provide a suitable compromise between the accuracy in predicting enthalpies and barriers for the β-scission reactions and computational cost.

We find that determination of the lowest-energy conformers of the $•OCH_2CH=O$ (**a1**), $•OCH(CH_3)CH=O$ (**a2**), $•OCH(CH_3)C(NH_2)=O$ (**a3**), and $•OC(CH_3)(NHCH=O)CH=O$ (**a4**) substituted alkoxy radicals is sensitive to the method used to optimize geometries. We have selected the conformer optimized with B3-LYP/6-311+G(3df,2p) that gives the lowest CCSD(T) energy for use in subsequent calculations.

In the calculation of enthalpies and barriers, we find that G3(MP2)//B3-LYP and G3X(MP2)-RAD give similar accuracy to more expensive high-level methods. However, these methods are still computationally too demanding to be used routinely with currently available resources for systems significantly larger than the largest models used in the present study, i.e., reactions A3 and A4. Cost-effective alternative methods are UB3-LYP/6-311+G(3df,2p)//UB3-LYP/6-31G(d) and RB3-LYP/6-311+G(3df,2p)//UB3-LYP/6-31G(d) or UBMK/6-311+G(3df,2p) and RBMK/6-311+G-(3df,2p) with either UB3-LYP/6-31G(d) or UBMK/6-31G(d) geometries. These give reasonable estimates of enthalpies and barriers that are within about 15 kJ mol^{-1} of the reference G3//B3-LYP values.

Heats of formation for each of the species involved in the four reactions under study were also calculated. The high-level methods perform well for the three species for which experimental values are available for comparison. U-CBS-QB3 seems to underestimate the heats of formation when compared with the other high-level methods. Predicted heats of formation at 0 K for the alkoxy radicals are −71.4 ($•OCH_2CH=O$, **a1**), −102.5 ($•OCH(CH_3)CH=O$, **a2**), −176.6 ($•OCH(CH_3)C(NH2)=O$, **a3**), and −264.6 ($•OC(CH_3)(NHCH=O)CH=O$, **a4**) kJ mol^{-1}. For the fragmentation products, $NH_2C(•)=O$ (**fp4**), and $CH(=O)NHC(CH_3)=O$ (**fp5**), we predict the respective values of −5.3 kJ mol^{-1} and −351.6 kJ mol^{-1}.

Acknowledgment. We gratefully acknowledge generous allocations of computer time from the ANU Supercomputing Facility, the Australian Partnership for Advanced Computing (APAC), and the Australian Centre for Advanced Computing and Communications (AC3) as well as the awards of an Australian Research Council Discovery Grant (to L.R.) and an Australian Postgraduate Award (to G.P.F.W.). We also thank Professor Jan Martin for making the BMK functional available for our use. L.R. is a member of the ARC Centre of Excellence for Free Radical Chemistry and Biotechnology.

Supporting Information Available: B3-LYP/6-311+G(3df,2p) GAUSSIAN archive entries of equilibrium and transition structures (Table S1). This material is available free of charge via the Internet at http://pubs.acs.org.

References

(1) Davies, M. J.; Dean, R. T. *Radical-Mediated Protein Oxidation: from Chemistry to Medicine*; Oxford University Press: Oxford; New York, 1997; and references therein.

(2) Dean, R. T.; Fu, S.; Stocker, R.; Davies, M. J. *Biochem. J.* **1997**, *324*, 1−18.

(3) Brunelle, P.; Rauk, A. *J. Alzheimer's Dis.* **2002**, *4*, 283−289. (b) Rauk. A. *Can. Chem. News* **2001**, *53*, 20−21. (c) Rauk A.; Armstrong D. A.; Fairlie D. P. *J. Am. Chem. Soc.* **2000**, *122*, 9761−9767.

(4) Gray, P.; Williams, A. *Chem. Rev.* **1959**, *59*, 239−328.

(5) Kochi, J. K. *J. Am. Chem. Soc.* **1962**, *84*, 1193−1197.

(6) Zhang, W.; Dowd, P. *Tetrahedron* **1993**, *49*, 1965−1978.

(7) Wilsey, S.; Dowd, P.; Houk, K. N. *J. Org. Chem.* **1999**, *64*, 8801−8811.

(8) Rauk, A.; Boyd, R. J.; Boyd, S. L.; Henry, D. J.; Radom, L. *Can. J. Chem.* **2003**, *81*, 431−442.

(9) Hippler, H.; Striebel, F.; Viskolcz, B. *Phys. Chem. Chem. Phys.* **2001**, *3*, 2450−2458. (b) Fittschen, C.; Hippler, H.; Viskolcz, B. *Phys. Chem. Chem. Phys.* **2000**, *2*, 1677−1683.

(10) Dibble, T. S. *J. Phys. Chem. A* **1999**, *103*, 8559−8565.

(11) Huang, M. L.; Rauk, A. *J. Phys. Org. Chem.* **2004**, *17*, 777−786.

(12) Shapley, W. A.; Bacskay, G. B. *J. Phys. Chem A* **1999**, *103*, 4514−4524.

(13) Song, K.-S.; Cheng, Y.-H.; Fu, Y.; Liu, L.; Li, X.-S.; Guo, Q.-X. *J. Phys. Chem. A* **2002**, *106*, 6651−6658.

(14) Hehre, W. J.; Radom, L.; Schleyer, P. v. R.; Pople, J. A. *Ab Initio Molecular Orbital Theory*; Wiley: New York, 1986.

(15) Koch, W.; Holthausen, M. C. *A Chemist's Guide to Density Functional Theory*; Wiley-VCH: Weinheim, 2000.

(16) Stanton, J. F.; Gauss, J.; Watts, J. D.; Nooijen, M.; Oliphant, N.; Perera, S. A.; Szalay, P. G.; Lauderdale, W. J.; Kucharski, S. A.; Gwaltney, S. R.; Beck, S.; Balková A.; Bernholdt, D. E.; Baeck, K. K.; Rozyczko, P.; Sekino, H.; Hober, C.; Bartlett, R. J. ACES II; Quantum Theory Project, University of Florida: Gainsville, 1992.

(17) Frisch, M. J.; Trucks, G. W.; Schlegel, H. B.; Scuseria, G. E.; Robb, M. A.; Cheeseman, J. R.; Zakrzewski, V. G.; Montgomery, J. A., Jr.; Stratmann, R. E.; Burant, J. C.; Dapprich, S.; Millam, J. M.; Daniels, A. D.; Kudin, K. N.; Strain, M. C.; Farkas, O.; Tomasi, J.; Barone, V.; Cossi, M.; Cammi, R.; Mennucci, B.; Pomelli, C.; Adamo, C.; Clifford, S.; Ochterski, J.; Petersson, G. A.; Ayala, P. Y.; Cui, Q.; Morokuma, K.; Malick, D. K.; Rabuck, A. D.; Raghavachari, K.; Foresman, J. B.; Cioslowski, J.; Ortiz, J. V.; Stefanov, B. B.; Liu, G.; Liashenko, A.; Piskorz, P.; Komaromi, I.; Gomperts, R.; Martin, R. L.; Fox, D. J.; Keith, T.; Al-Laham, M. A.; Peng, C. Y.; Nanayakkara, A.; Gonzalez, C.; Challacombe, M.; Gill, P. M. W.; Johnson, B.; Chen, W.; Wong, M. W.; Andres, J. L.; Head-Gordon, M.; Replogle, E. S.; Pople, J. A. GAUSSIAN 98, Revision A.11.3; Gaussian Inc.: Pittsburgh, PA, 1998.

(18) Frisch, M. J.; Trucks, G. W.; Schlegel, H. B.; Scuseria, G. E.; Robb, M. A.; Cheeseman, J. R.; Montgomery, J. A., Jr.; Vreven, T.; Kudin, K. N.; Burant, J. C.; Millam, J. M.; Iyengar, S. S.; Tomasi, J.; Barone, V.; Mennucci, B.; Cossi, M.; Scalmani, G.; Rega, N.; Petersson, G. A.; Nakatsuji, H.; Hada, M.; Ehara, M.; Toyota, K.; Fukuda, R.; Hasegawa, J.; Ishida, M.; Nakajima, T.; Honda, Y.; Kitao, O.; Nakai, H.; Klene, M.; Li, X.; Knox, J. E.; Hratchian, H. P.; Cross, J. B.; Adamo, C.; Jaramillo, J.; Gomperts, R.; Stratmann, R. E.; Yazyev, O.; Austin, A. J.; Cammi, R.; Pomelli, C.; Ochterski, J. W.; Ayala, P. Y.; Morokuma, K.; Voth, G. A.; Salvador, P.; Dannenberg, J. J.; Zakrzewski, V. G.; Dapprich, S.; Daniels, A. D.; Strain, M. C.; Farkas, O.; Malick, D. K.; Rabuck, A. D.; Raghavachari, K.; Foresman, J. B.; Ortiz, J. V.; Cui, Q.; Baboul, A. G.; Clifford, S.; Cioslowski, J.; Stefanov, B. B.; Liu, G.; Liashenko, A.; Piskorz, P.; Komaromi, I.; Martin, R. L.; Fox, D. J.; Keith, T.; Al-Laham, M. A.; Peng, C. Y.; Nanayakkara, A.; Challacombe, M. Gill, P. M. W.; Johnson, B.; Chen, W.; Wong, M. W.; Gonzalez, C.; and Pople, J. A. Gaussian 03, Revision B.03; Gaussian, Inc.: Pittsburgh, PA, 2003.

(19) Amos, R. D.; Bernhardsson, A.; Berning, A.; Celani, P.; Cooper, D. L.; Deegan, M. J. O.; Dobbyn, A. J.; Eckert, F.; Hampel, C.; Hetzer, G.; Knowles, P. J.; Korona, T.; Lindh, R.; Lloyd, A. W.; McNicholas, S. J.; Manby, F. R.; Meyer, W.; Mura, M. E.; Nicklass, A.; Palmieri, P.; Pitzer, R.; Rauhut, G.; Schutz, M.; Schumann, U.; Stoll, H.; Stone, A. J.; Tarroni, R.; Thorsteinsson, T.; Werner, H.-J. *MOLPRO 2002.6*; University of Birmingham: Birmingham, U.K., 2002.

(20) Knowles, P. J.; Hampel, C.; Werner, H.-J. *J. Chem. Phys.* **1993**, *99*, 5219−5227.

(21) Baboul, A. G.; Curtiss, L. A.; Redfern, P. C.; Raghavachari, K. *J. Chem. Phys.* **1999**, *110*, 7650−7657.

(22) Gonzalez, C.; Schlegel, H. B. *J. Chem. Phys.* **1989**, *90*, 2154−2161.

(23) Gonzalez, C.; Schlegel, H. B. *J. Phys. Chem.* **1990**, *94*, 5523−5527.

(24) Boese, D. A.; Martin, J. M. L. *J. Chem. Phys.* **2004**, *121*, 3405−3416.

(25) Scott, A. P.; Radom, L. *J. Phys. Chem.* **1996**, *100*, 16502−16513.

(26) Curtiss, L. A.; Redfern, P. C.; Raghavachari, K.; Pople, J. A. *J. Chem. Phys.* **2001**, *114*, 108−117.

(27) Lynch, B. J.; Truhlar, D. A. *J. Phys. Chem A* **2001**, *105*, 2936−2941.

(28) Montgomery, J. A., Jr.; Frisch, M. J.; Ochterski, J. W.; Petersson, G. A. *J. Chem. Phys.* **1999**, *110*, 2822−2827.

(29) U-CBS-QB3 is a variant of CBS-QB3 that omits the empirical correction for spin contamination in the unrestricted wave function. See, for example: (a) Gómez-Balderas, R.; Coote, M. L.; Henry, D. J.; Radom, L. *J. Phys. Chem. A*, **2004**, *108*, 2874−2883. (b) Wood, G. P. F.; Henry, D. J.; Radom, L. *J. Phys. Chem. A* **2003**, *107*, 7985−7990. (c) Coote, M. L. *J. Phys. Chem. A* **2004**, *108*, 3865−3872.

(30) Henry, D. J.; Sullivan, M. B.; Radom, L. *J. Chem. Phys.* **2003**, *118*, 4849−4860.

(31) Martin, J. M. L.; De Oliveira, G. J. *J. Chem. Phys.* **1999**, *111*, 1843−1856.

(32) Bataev, V. A.; Abramenkov, A. V.; Godunov, I. A. *Russ. Chem. Bull.* **2001**, *50*, 945−951.

(33) (a) Von Neumann, J.; Wigner, E. *Z. Phys.* **1929**, *30*, 467 (b) Stanton, J. F. *J. Chem. Phys.* **2001**, *115*, 10382−10393, and references therein. (c) Russ, N. J.; Crawford, D. T.; Tschumper, G. S. *J. Chem. Phys.* **2004**, *120*, 7298−7306.

(34) See, for example: Coote, M. L.; Wood, G. P. F.; Radom, L. *J. Phys. Chem. A* **2002,** *106*, 12124−12138.

(35) Curtiss, L. A.; Raghavachari, K.; Redfern, P. C.; Pople, J. A. *J. Chem. Phys.* **2000**, *112*, 7374−7383.

(36) Heats of formation in (0 K, kJ mol^{-1}) calculated with UBMK/6-311+G(3df,2p)//UBMK/6-31G(d) are as follows: −113.4 (CH_2═O, **fp1**), −114.1 (CH_3CH═O, **fp2**), 25.7 (•CH═O, **fp3**), −42.6 (NH_2C(•)═O, **fp4**), −393.4 (CH(═O)NHC-(CH_3)═O, **fp5**), −100.8 (•OCH_2CH═O, **a1**), −131.5 (•OCH-(CH_3)CH═O, **a2)**, −222.0 (•OCH(CH_3)C(NH2)═O, **a3)**, and −312.0 (•$OC(CH_3)$(NHCH═O)CH═O, **a4**).

(37) (a) Parthiban, S.; Martin, J. M. L. *J. Chem. Phys.* **2001**, *114*, 6014−6029. (b) Boese, D. A.; Oren, M.; Atasoylu, O.; Martin, J. M. L.; Kállay, M.; Gauss. J. *J. Chem. Phys.* **2004**, *120*, 4129−4141.

(38) Fletcher, R. A.; Pilcher, G. *Trans. Faraday Soc.* **1970**, *66*, 794−799.

(39) Lias, S. G.; Bartmess, J. E.; Liebman, J. F.; Holmes, J. L.; Levin, R. D.; Mallard, W. G. *J. Phys. Chem. Ref. Data* **1988**, *17*, Suppl 1.

(40) Feller, D.; Dixon, D. A.; Francisco, J. S. *J. Phys. Chem. A* **2003**, *107*, 1604−1617.

(41) Henry, D. J.; Parkinson, C. J.; Radom, L. *J. Phys. Chem. A* **2002**, *106*, 7927−7936.

(42) Becerra, R.; Carpenter, I. W.; Walsh, R. *J. Phys. Chem. A* **1997**, *101*, 4185−4190. The reported $\Delta_f H_{298}$ value has been back-corrected to 0 K: see Henry et al.[41]

(43) Berkowitz, J.; Ellison, G. B.; Gutman, D. *J. Phys. Chem.* **1994**, *98*, 2744−2765.

CT050133G